

University of Alabama in Huntsville

**LOUIS**

---

Honors Capstone Projects and Theses

Honors College

---

4-28-2019

## **An Investigation of Iron Catalysts for the Oxidative Dehydrogenation of Ethane**

Courtney Nicole Anderson

Follow this and additional works at: <https://louis.uah.edu/honors-capstones>

---

### **Recommended Citation**

Anderson, Courtney Nicole, "An Investigation of Iron Catalysts for the Oxidative Dehydrogenation of Ethane" (2019). *Honors Capstone Projects and Theses*. 15.  
<https://louis.uah.edu/honors-capstones/15>

This Thesis is brought to you for free and open access by the Honors College at LOUIS. It has been accepted for inclusion in Honors Capstone Projects and Theses by an authorized administrator of LOUIS.

# An Investigation of Iron Catalysts for the Oxidative Dehydrogenation of Ethane

by

**Courtney Nicole Anderson**

**An Honors Capstone**

**submitted in partial fulfillment of the requirements**

**for the Honors Diploma**

**to**

**The Honors College**

**of**

**The University of Alabama in Huntsville**

**April 23, 2019**

**Honors Capstone Director: Dr. Yu Lei**

**Associate Professor of Chemical and Materials Engineering**

Courtney Anderson      04/23/2019  
Student (signature)      Date

Yu Lei      4/24/2019  
Director (signature)      Date

Anneadhas      4/20/2019  
Department Chair (signature)      Date

K. J.      5/1/19  
Honors College Dean (signature)      Date



Honors College  
Frank Franz Hall  
+1 (256) 824-6450 (voice)  
+1 (256) 824-7339 (fax)  
honors@uah.edu

### Honors Thesis Copyright Permission

This form must be signed by the student and submitted as a bound part of the thesis.

In presenting this thesis in partial fulfillment of the requirements for Honors Diploma or Certificate from The University of Alabama in Huntsville, I agree that the Library of this University shall make it freely available for inspection. I further agree that permission for extensive copying for scholarly purposes may be granted by my advisor or, in his/her absence, by the Chair of the Department, Director of the Program, or the Dean of the Honors College. It is also understood that due recognition shall be given to me and to The University of Alabama in Huntsville in any scholarly use which may be made of any material in this thesis.

Courtney Anderson

Student Name (printed)

Courtney Anderson

Student Signature

04/23/2019

Date

**Table of Contents**

Abstract	2
1. Introduction	3
2. Experimental Methods	4
2.1. Catalyst Synthesis	4
2.2. Catalyst Characterization	5
2.3. Catalyst Evaluation	6
3. Results and Discussion	7
3.1. Catalyst Characterization	7
3.2. Catalyst Performance	14
4. Conclusions and Future Work	17
References	18
Appendix	20

**Abstract**

Ethylene is a highly-demanded chemical intermediate that is used to synthesize many plastics. Over 134 million tons of ethylene are produced annually,<sup>1</sup> but the current industrial method of producing ethylene via ethane steam cracking is highly energy intensive. The oxidative dehydrogenation (ODH) of ethane has gained attention because this process is exothermic and has the potential to greatly reduce energy costs associated with production. The current downfall of this process is its low ethylene yield. We are proposing that an iron-doped silica-supported catalyst can increase conversion and selectivity in the ODH reaction. We developed a recipe for a high surface area iron-doped catalyst (named FS-1 for iron silicalite-1). The introduction of iron into the silicalite framework is characterized using XRD, BET, and XAS. FS-1 has a surface area of 404 m<sup>2</sup>/g. Iron is positioned in isolated sites within the silicalite matrix and has an oxidation state resembling Fe<sub>2</sub>O<sub>3</sub>. Conversion and selectivity of the FS-1 catalyst were measured using TCD gas chromatography. We tested performance dependence on concentration of iron in the support, and the 1:100 Fe:Si molar ratio sample was found to have the highest yield at 4.94% ± 0.016%.

### 1. Introduction

Ethylene is the most important chemical building block in the plastics industry. It is the prerequisite for polyethylene, which is used to make plastic bottles and bags; PVC, which is used for piping and construction; and polystyrene, which is used to make styrofoam. Approximately 134 million tons of ethylene are produced annually.<sup>[1]</sup> As fracking increases, the amount of available ethane feedstock increases. Steam cracking is the current industrial method for producing ethylene from ethane. The reaction is shown in Equation 1. This reaction is extremely endothermic and requires a lot of energy. In addition to requiring a lot of energy, steam cracking causes a lot of coke buildup on the inner walls of the reactor, so the process must be shut down for frequent cleanings.<sup>[2]</sup>



The ethane oxidative dehydrogenation (ODH) reaction, shown in Equation 2, is more economical because it is exothermic, so it creates heat that can be used to generate electricity or drive other processes in the chemical plant. However, total oxidation can also occur in the presence of oxygen, as shown in Figure 1.<sup>[3]</sup> Total oxidation generates undesirable products CO and CO<sub>2</sub>. The challenge is to find a catalyst that selects for ethylene and not the total oxidation products.

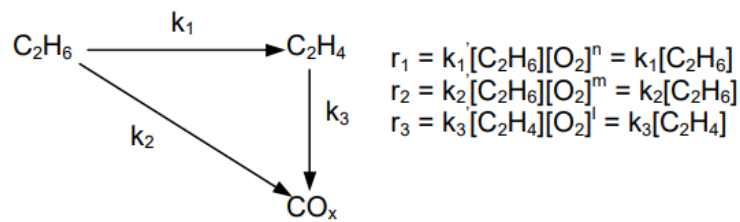


Figure 1. Reaction pathways for ethane ODH.

The current most effective catalysts for this reaction are a cocktail of several elements, such as Mo/V/Te(Sb)/Nb/O or Li/Dy/Mg/O. These catalysts have yields near 80%,<sup>[4]</sup> though their composition makes them expensive to produce. By comparison, a catalyst made of iron would be much more cost effective since iron is one of the most abundant elements in the Earth's crust.<sup>[5]</sup> Iron is known to form catalytic complexes that select for lightweight hydrocarbons.<sup>[6]</sup> We hypothesize that a single-site iron support structure will facilitate monodentate absorption and allow the C-C bonds to remain intact.

## 2. Experimental Methods

### 2.1. Catalyst Synthesis

To generate iron silicalite-1 (FS-1), 2 g Tween 20 (Sigma), 20 mL deionized water, 27 mL TPAOH (Acros Chemicals, 25% in water), and 40 mL TEOS (Aldrich, reagent grade 98%) were mixed vigorously for 1 h. Next, a solution of 25 mL isopropanol (Acros) and an appropriate molar ratio of ferrocene (Aldrich, 98%) (see Table 1 for mass values) are added dropwise to the mixing solution. After the solution mixes for another hour, the solution is transferred to a Teflon-lined stainless-steel autoclave and kept under autogenous pressure at 170 °C for 18 h.

Table 1. Mass of Ferrocene to Achieve Desired Ratios. Calculations based on using 40 mL of 98% tetraethylorthosilicate as silica source (0.176 mol silica).

<i>Fe:Si Ratio</i>	<i>Fe needed (moles)</i>	<i>Ferrocene (g)</i>
<i>1:50</i>	0.00352	0.6549
<i>1:75</i>	0.00264	0.4911
<i>1:100</i>	0.00176	0.3273
<i>1:200</i>	0.00088	0.1637
<i>1:400</i>	0.00044	0.0819

Next, the white solids are separated from the brown liquid through centrifugation in an IEC Spinette Centrifuge (Manual IM-183). There should be enough product formed to fill four 15 mL centrifugation tubes fully and four more centrifugation tubes to 8-9 mL. The partially filled tubes are filled the rest of the way with DI water that was used to rinse the residue off the Teflon lining. Achieving good separation of the solid and liquid layers takes around an hour. The liquid layer is disposed of and the remaining white solid is washed with DI water. The DI water/solid solution is separated in the centrifuge for around one hour. The water layer is disposed of, and the remaining solids are placed in a vacuum chamber to dry at room temperature. The drying process takes between 1 and 4 days. Once dry, samples are calcined in a Lindberg tube furnace in ambient air at 550 °C for 4 h.

## **2.2. Catalyst Characterization**

X-ray diffraction (XRD) measurements were carried out using a Rigaku MiniFlex 600 powder X-ray diffractometer. The diffractometer was operated at 40 kV and 15 mA using Cu radiation with a characteristic wavelength of 0.1542 nm.  $2\theta$  data was collected between 10° and 90° with a scanning speed of 0.5°/min and a step size of 0.05°. Brunauer-Emmett-Teller (BET) isotherm data was measured using nitrogen adsorption at 77 K in a Quantachrome gas sorption device (model ASIQC0000000-6). X-ray absorption spectroscopy (XAS) data was collected from the Advanced Photon Source synchrotron at Argonne National Laboratory. X-ray absorption near edge structure (XANES) and extended X-ray absorption fine structure (EXAFS) were plotted to determine the isolation of iron in the silica matrix. Both the XANES and EXAFS data sets were normalized to a step height of 1.

### 2.3. Catalyst Evaluation

The catalyst was tested in a tube reactor, and performance data was obtained from a thermal conductivity detector (TCD) gas chromatograph. The experimental setup is pictured in Figure 2. 50 mg of catalyst were sieved to between 180 and 250  $\mu\text{m}$  in diameter. The catalyst was diluted in 500 mg of crushed quartz to prevent hot spots from occurring in the tube reactor. The tube reactor consisted of a quartz tube with the diluted catalyst suspended in the center between two plugs of glass wool. Mass flow meters set the overall gas flowrate through the tube to 50 sccm, consisting of 6% oxygen, 18% ethane, and the remainder as helium. Helium serves as the inert so that the gas chromatograph does not get oversaturated. The furnace was set to a ramping up to 550  $^{\circ}\text{C}$  at 35  $^{\circ}\text{C}/\text{min}$ , and maximum temperature was held for 160 minutes. The ramping profile is shown in Figure 3. Gas chromatograph measurements were taken every 20 minutes.



Figure 2. Performance testing setup.

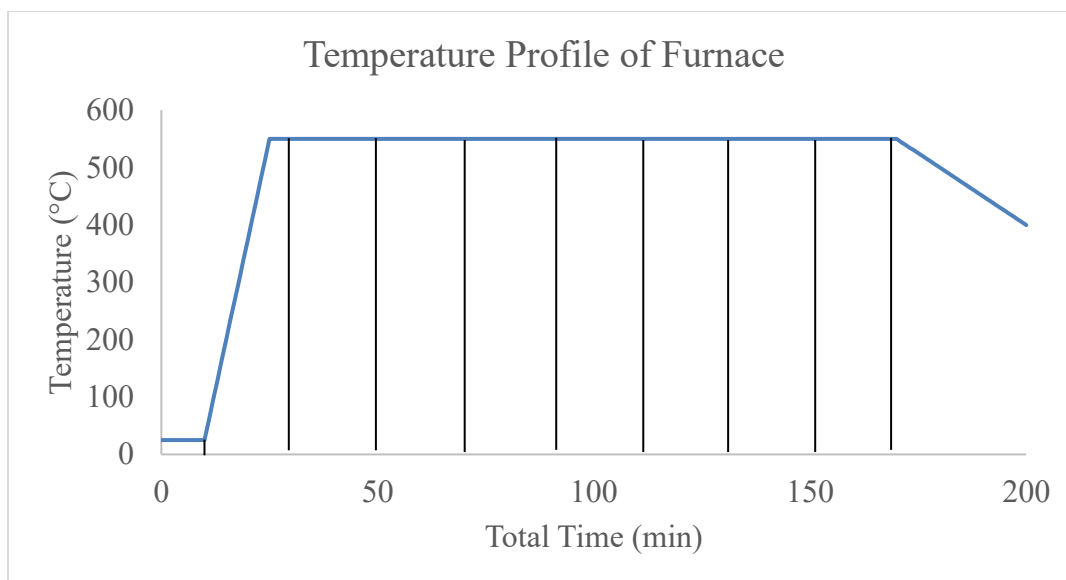


Figure 3. Temperature Profile of Furnace. Vertical black lines represent times when TCD measurements were taken.

Based on the relative gas amounts measured by the TCD gas chromatograph, the following equations can be used to characterize catalyst performance. Equation 3 solves for conversion, the percentage of ethane feed that is converted to product. Equation 4 solves for selectivity, the percentage of product that is our desired product, ethylene. Equation 5 solves for yield, the percentage of ethylene formed per mole of ethane feed.

$$\text{conversion} = \frac{\text{moles of ethane in feed} - \text{moles of ethane in product}}{\text{moles of ethane in feed}} * 100 \quad (3)$$

$$\text{selectivity} = \frac{\text{moles of ethylene}}{\text{moles of } \left( \text{ethylene} + \left( \frac{1}{2} \right) (\text{CO}_2 + \text{CO} + \text{CH}_4) \right)} * 100 \quad (4)$$

$$\text{yield} = \text{conversion} * \text{selectivity} \quad (5)$$

### 3. Results and Discussion

#### 3.1. Catalyst Characterization

The unit cell volume of the FS-1 matrix was determined using XRD. Figure 4 shows the full XRD spectrum, while Figure 5 zooms in on the peaks of interest for the 1:50 and 1:400 ratio

samples. The S-1 matrix is known to have an orthorhombic structure,<sup>[7]</sup> so the samples were expected to have 3 characteristic peaks corresponding to Miller indices of [1 5 0], [5 1 1], and [2 5 0]. Table 1 shows the lattice parameter calculations based on peak angles. The increase in cell volume due to calcination is  $1.29 \pm 0.67 \text{ nm}^3$ , and the change in volume increases as the iron loading of the matrix increases. A complete table of all the intermediate values needed to calculate the lattice parameters is given in the Appendix.

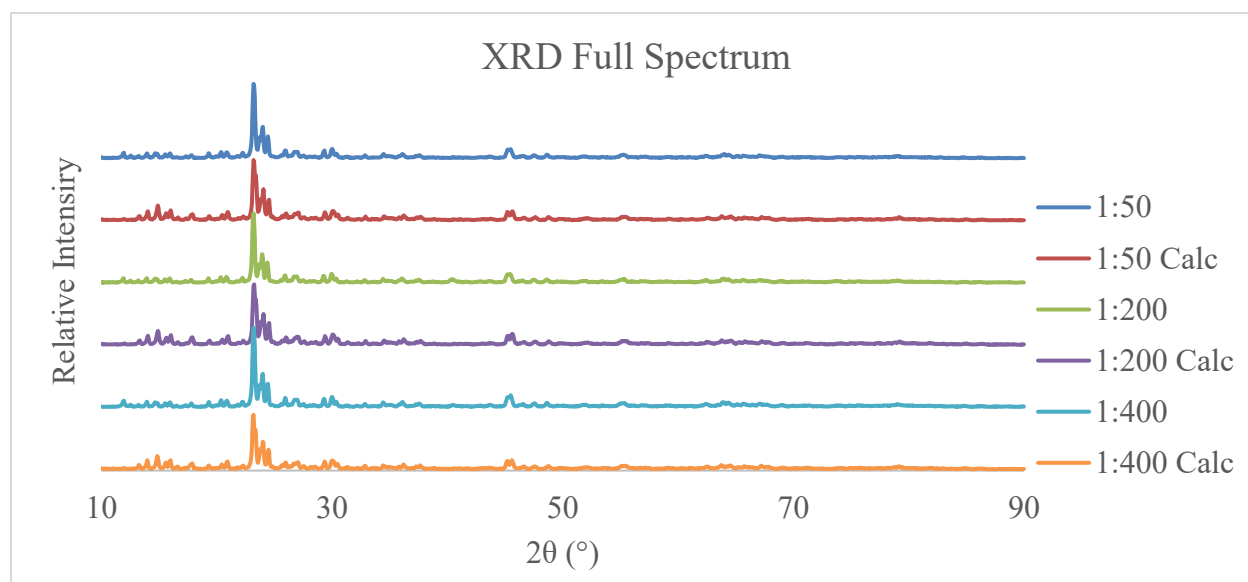


Figure 4. The XRD peaks are shown for uncalcined and calcined samples of Fe:Si ratio 1:50, 1:200, and 1:400.

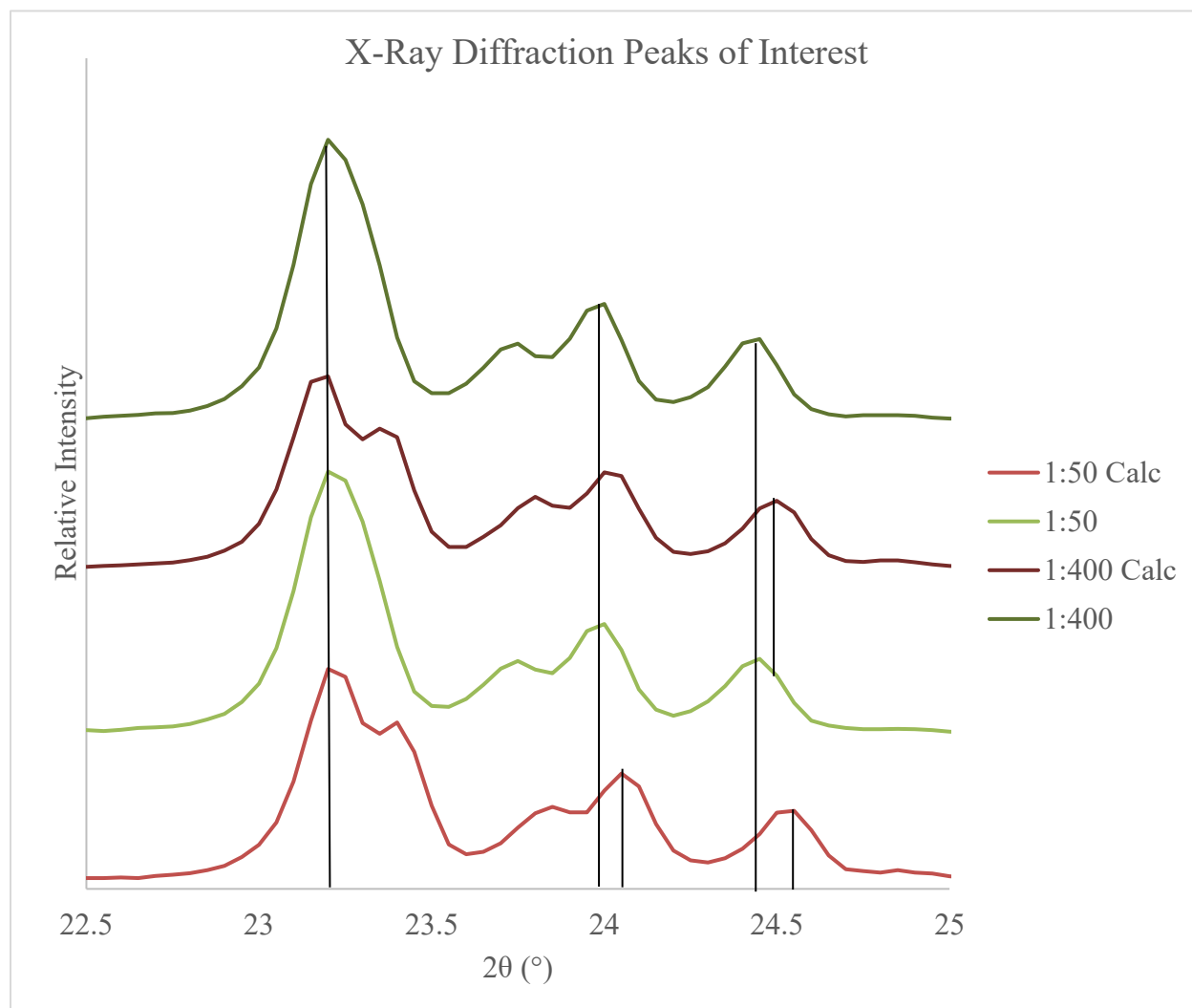


Figure 5. This figure zooms in on the three characteristic peaks of the 1:50 and 1:400 molar ratio uncalcined and calcined samples.

Black vertical lines were drawn to show the peak shift between the uncalcined and the calcined samples. No shift occurs in the first peak, though the 1:50 molar ratio sample shows a shift in the second peak and both samples show a shift in the third peak. A shift to the right means that the lattice parameter increases, and therefore, the unit cell volume increases.

Table 1. Calculated lattice parameters and unit cell volumes based on XRD measurements.

	$2\theta$	<i>Lattice Parameter</i>		$V$ ( $\text{nm}^3$ )
<i>1:50</i>	23.2	2.012	a	4.306
	24	1.953	b	
	24.45	1.096	c	
<i>1:50 Calcined</i>	23.2	1.934	a	6.339
	24.05	1.956	b	
	24.55	1.676	c	
<i>1:200</i>	23.2	2.054	a	3.902
	23.95	1.951	b	
	24.4	0.973	c	
<i>1:200 Calcined</i>	23.25	1.970	a	4.977
	24.05	1.950	b	
	24.55	1.296	c	
<i>1:400</i>	23.2	2.012	a	4.306
	24	1.953	b	
	24.45	1.096	c	
<i>1:400 Calcined</i>	23.2	1.972	a	5.062
	24	1.954	b	
	24.5	1.313	c	

The BET adsorption and desorption curves are presented in Figure 6. The SinglePoint and MultiPoint BET both yielded surface areas around 404  $\text{m}^2/\text{g}$  for the 1:100 molar ratio sample. A catalyst with high surface area usually has a higher activity because more reactants can be absorbed by the catalyst structure. The 1:100 molar ratio sample had a pore radius of 17.09 Å and a pore volume of 0.3818  $\text{cm}^3/\text{g}$ .

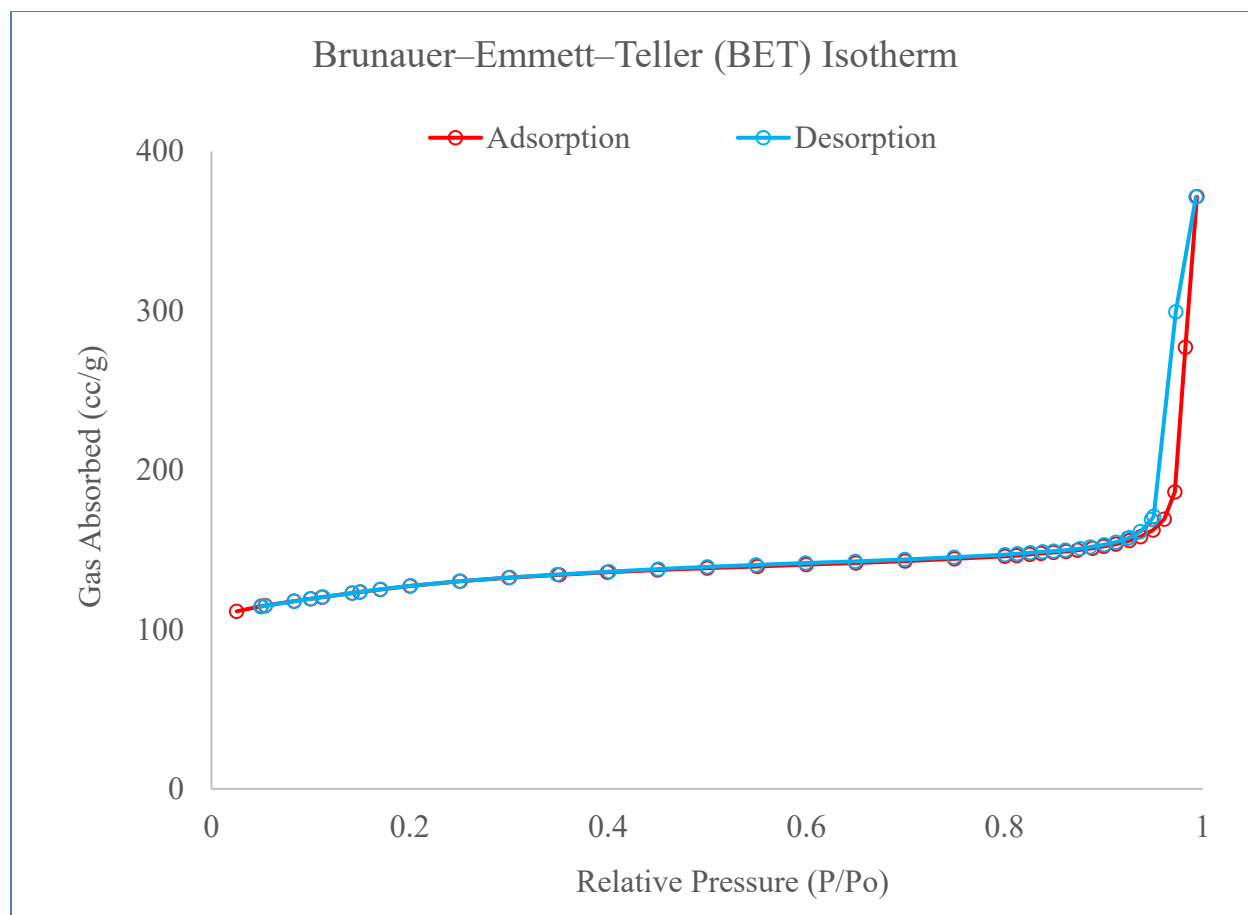


Figure 6. 38 adsorption measurements and 37 desorption measurements were taken using nitrogen at 77 K to obtain the BET isotherm curve.

XAS data is plotted in Figure 7 and Figure 8. The XANES compares the electronic structure of iron in an FS-1 sample to iron in its common oxidation states. The positions of the slope leading up to the peak will be identical in samples with the same oxidation state. A black line is drawn through the peak of the FeO curve to show that it does not line up with the peaks of the other samples. The inset in the upper corner of the graph compares FS-1 to its most similar curve, Fe<sub>2</sub>O<sub>3</sub>. Though the peaks differ in sharpness, the precise lineup of the edges suggests that FS-1 contains iron in the Fe<sub>2</sub>O<sub>3</sub> oxidation state.

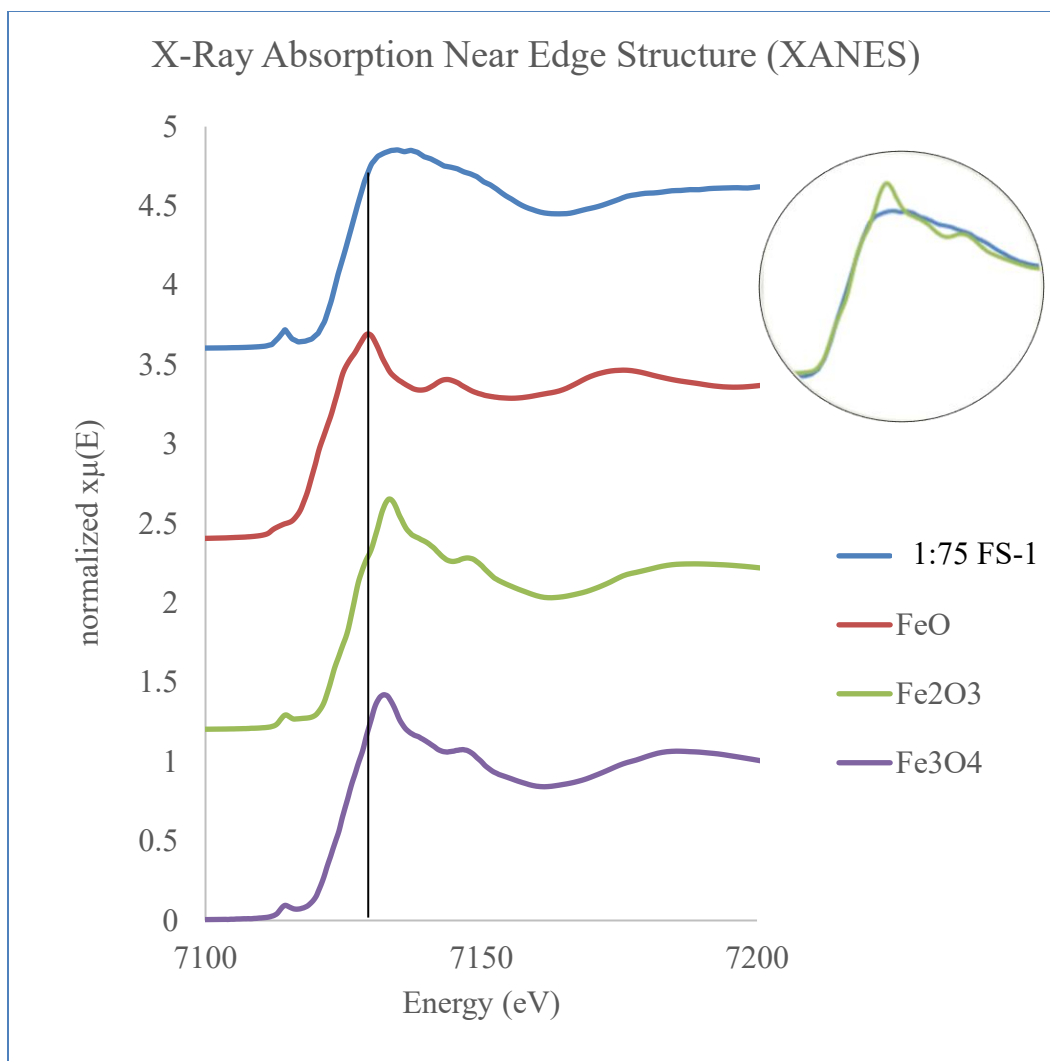


Figure 7. XANES plot comparing 1:75 FS-1 to FeO, Fe<sub>2</sub>O<sub>3</sub>, and Fe<sub>3</sub>O<sub>4</sub>

The EXAFS describes the molecules neighboring iron in the crystalline matrix. The first peak, present in all samples, is the Fe-O peak. It is to be expected that iron borders oxygen in all these samples because in FS-1, the S-1 matrix is made of SiO<sub>2</sub>. The second peak represents the Fe-O-Fe peak. The lack of this peak in FS-1 indicates that iron is isolated from other iron molecules in the FS-1 matrix.

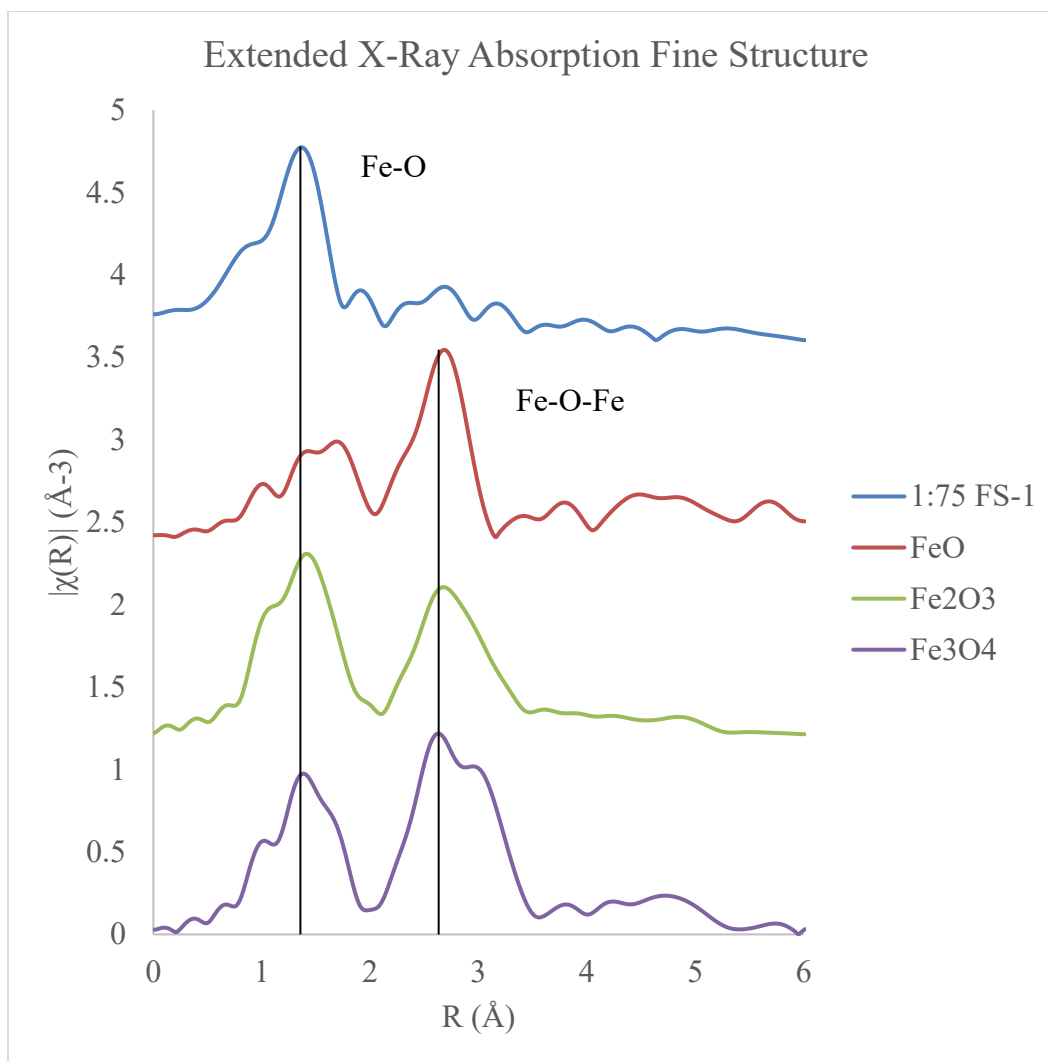


Figure 8. EXAFS plot comparing 1:75 FS-1 to FeO, Fe<sub>2</sub>O<sub>3</sub>, and Fe<sub>3</sub>O<sub>4</sub>

### 3.2. Catalyst Performance

Figure 10 shows conversion of ethane as a function of time for four of the FS-1 samples. The samples typically take 25 minutes at maximum temperature to reach a steady state conversion value. Conversion values are relatively low for all samples, ranging from 4.5 – 7.8% with the 1:100 sample having the highest conversion. Selectivity values range from 63 – 80% with the 1:50 sample having the highest selectivity. Conversion and selectivity values for all samples are tabulated in the Appendix.

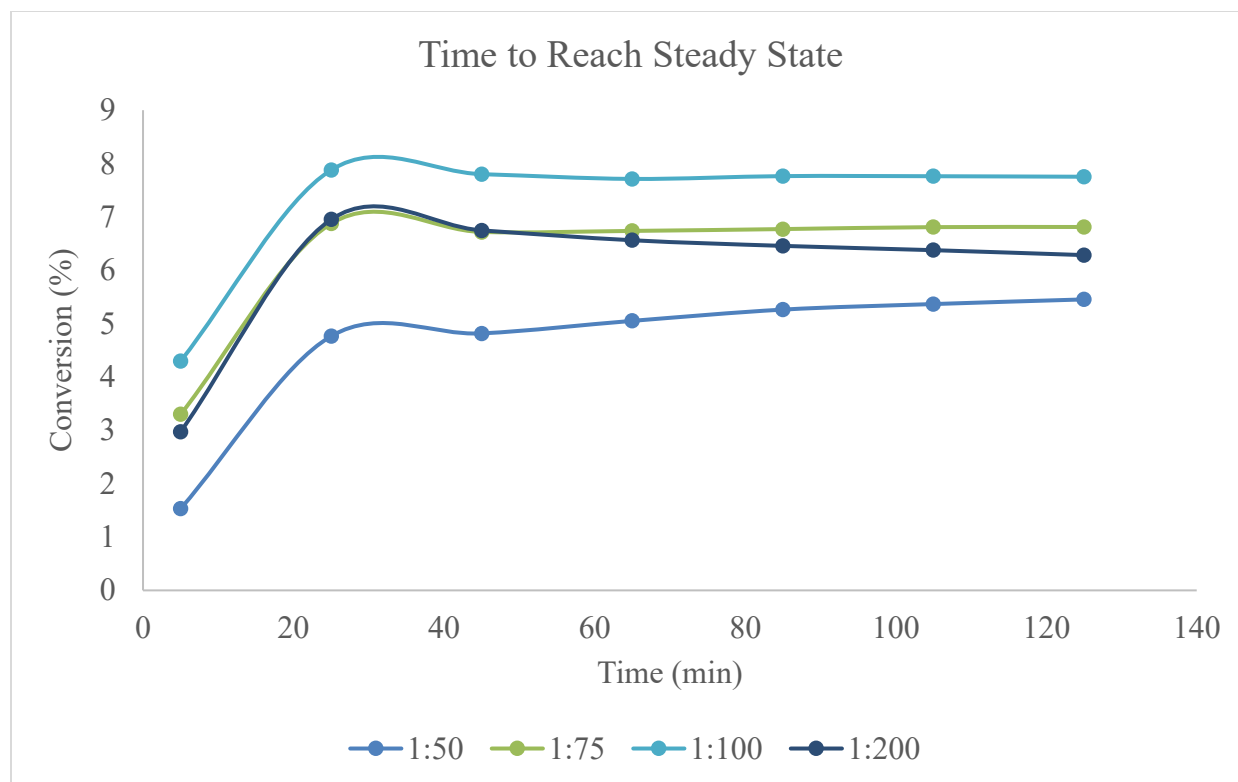


Figure 10. Conversion values took an average of 25 minutes to reach steady state values.

Since selectivity and conversion based on iron loading ratio showed conflicting trends, the product of selectivity and conversion (yield), was used to determine overall catalyst performance (see Figure 11). Average yield was taken over the 100 minutes that each sample was at steady state. The 1:100 sample had the highest yield at  $4.94\% \pm 0.016\%$ , likely due to an optimized number of isolated Fe sites. The 1:100 sample also had the most consistent performance as suggested by the small error bars. The formation rate of ethylene for the 1:100 sample was  $606 \text{ g ethylene (kg cat)}^{-1} \text{ hr}^{-1}$ . Values and assumptions used to calculate the formation rate can be found in the Appendix.

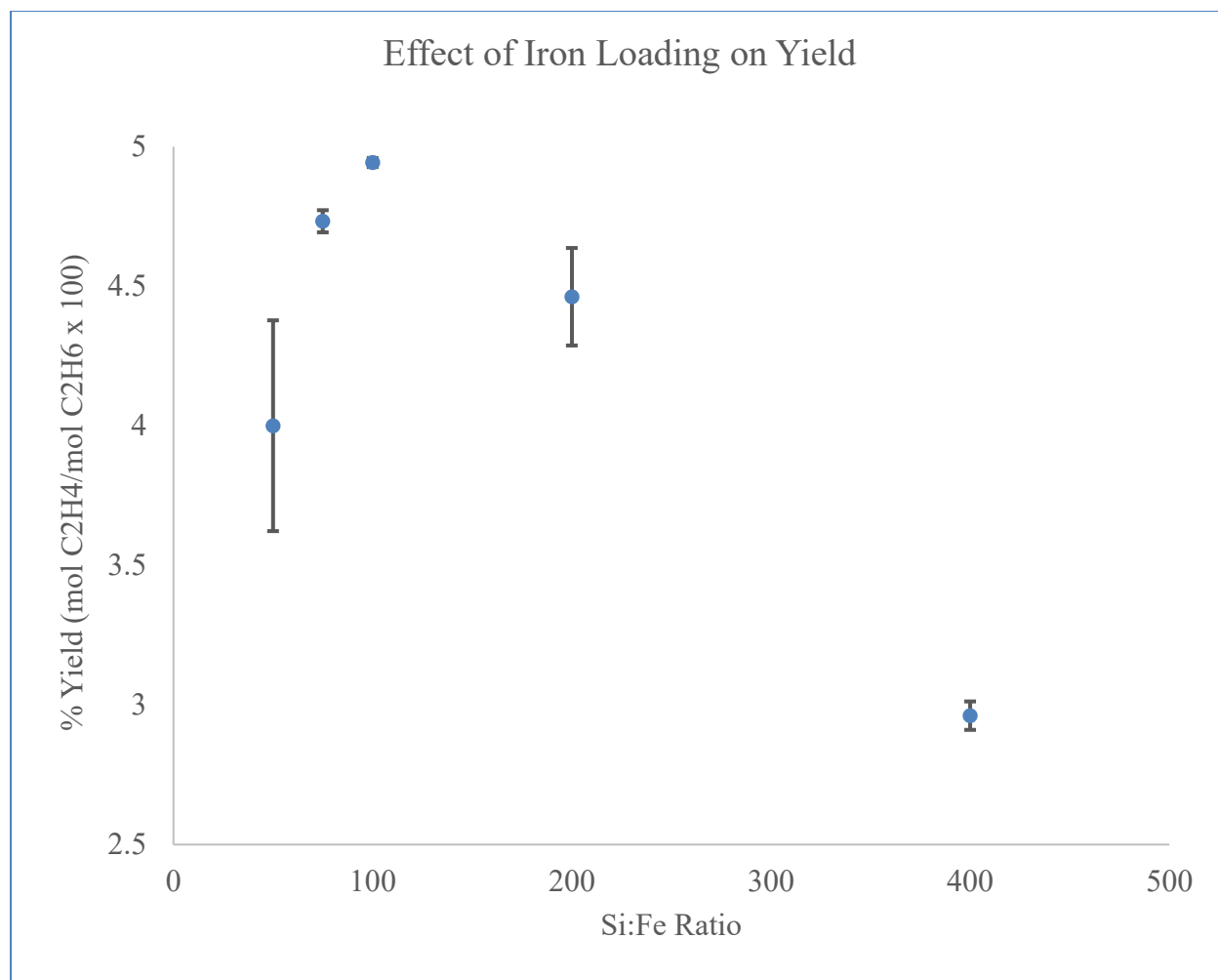


Figure 11. Yield of each of the five samples is plotted with error bars of  $\pm$  one standard deviation.

It is hypothesized that this catalyst is effective at selecting for ethylene because of its isolated iron structure. Figure 12 shows two proposed mechanisms for absorption of ethylene onto an iron catalyst. In the adjacent structure, ethylene absorbs via a bidentate mechanism (two iron atoms latch on to the ethylene molecule), and the C-C bond is vulnerable to breakage. In the isolated structure, ethylene absorbs via a monodentate mechanism, and the C-C bond can remain intact while oxygen removes the hydrogen atoms.

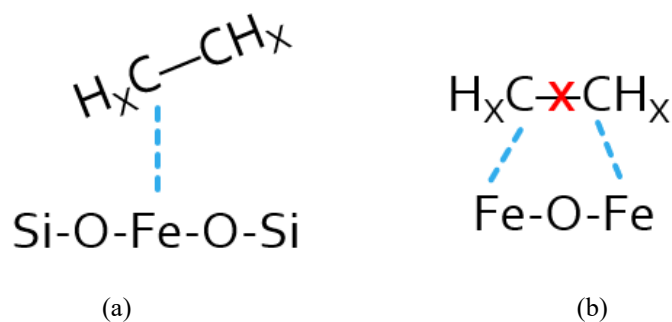


Figure 12. Proposed absorption mechanisms for (a) isolated iron and (b) adjacent iron)

When compared to literature, this catalyst has a lot of room for improvement. Figure 13<sup>[4]</sup> is a graph of selectivity versus conversion for a variety of ODH catalysts. Points 59 and 67, marked in blue, are catalysts from Cavani et. al's literature review that contain iron. Point 59 is Fe/P/O<sup>[8]</sup> and point 67 is La/Sr/Fe/Cl/O.<sup>[9]</sup> Our catalyst, plotted in red, has a comparable selectivity but lags far behind in conversion.

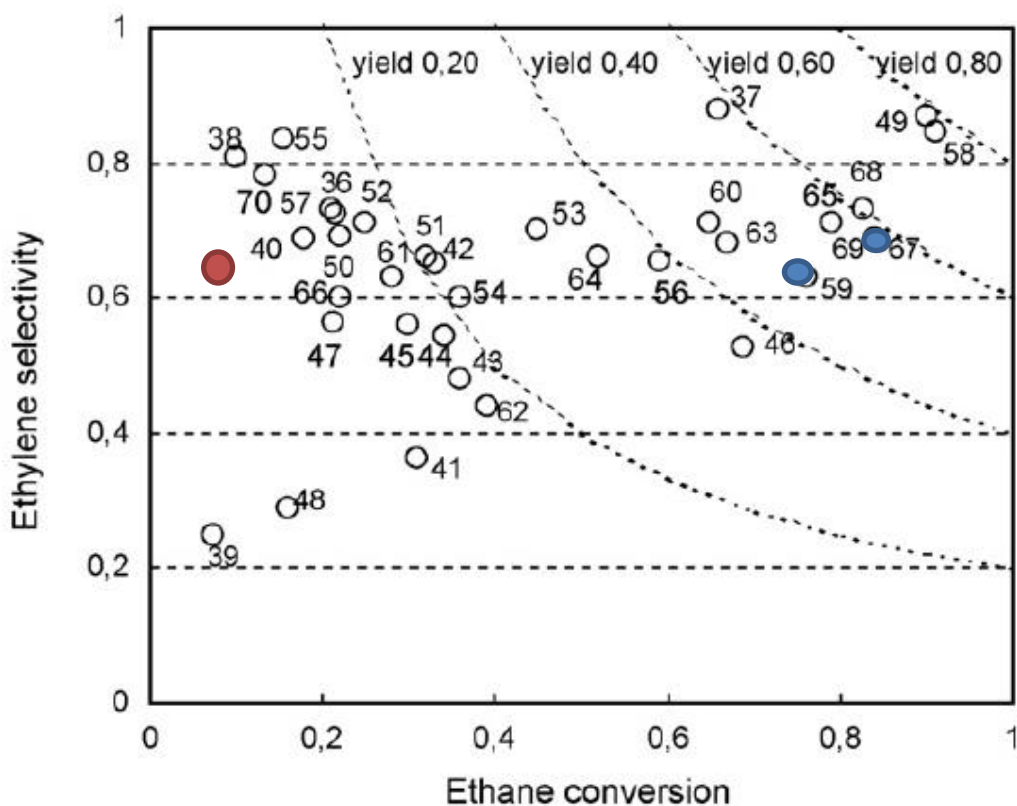


Figure 13. Comparison to literature values. Adapted from Cavani et. al.

#### 4. Conclusions and Future Work

A recipe for the synthesis of high surface area iron doped S-1 was developed. Iron exists in single sites isolated by the S-1 framework, as confirmed by XAS and XRD. 1:100 FS-1 exhibited the highest yield due to the optimized number of isolated Fe sites, though its performance is far behind that of multi-element catalysts. However, it is important to note that the reaction conditions for our catalyst have not been optimized. Though the 1:100 FS-1 performed best in this experiment, future experimentation is required to determine if the optimal loading is truly 1:100 or if it is somewhere nearby, like 1:90 or 1:120. Performance could also be improved by changing the composition of the feed or the temperature of the reaction.

It was hypothesized that the isolated iron matrix was effective due to a monodentate absorption mechanism, but a control experiment using an adjacent iron matrix is needed to prove this theory. Additionally, since  $\text{Fe}_2\text{O}_3$  is known to form catalytic complexes with gold, it is worth testing the performance of Au-doped FS-1 in a future experiment. This doping could be done via incipient wetness impregnation (IWI) or deposition precipitation (DP).

### References

- <sup>1</sup>Lazonby, J. (2017, January 4). Ethene (Ethylene). Retrieved April 9, 2019, from <http://www.essentialchemicalindustry.org/chemicals/ethene.html>
- <sup>2</sup>Ai-Zegbayer, Y., Mayman, S. A., & Ai-Smarei, T. (2010). Oxidative Dehydrogenation of Ethane to Ethylene Over Mo-V-Nb Catalysts: Effect of Calcination Temperature and Type of Support. *Journal of King Saud University - Engineering Sciences*, 22(1), 21-27. doi:10.1016/s1018-3639(18)30506-3
- <sup>3</sup>Argyle, M. D., Chen, K., Bell, A. T., & Iglesia, E. (2002). Effect of Catalyst Structure on Oxidative Dehydrogenation of Ethane and Propane on Alumina-Supported Vanadia. *Journal of Catalysis*, 208(1), 139-149. doi:10.1006/jcat.2002.3570
- <sup>4</sup>Cavani, F., Ballarini, N., & Cericola, A. (2007). Oxidative dehydrogenation of ethane and propane: How far from commercial implementation? *Catalysis Today*, 127(1-4), 113-131. doi:10.1016/j.cattod.2007.05.009
- <sup>5</sup>Frey, P. A., & Reed, G. H. (2012). The Ubiquity of Iron. *ACS Chemical Biology*, 7, 1477-1481. doi:dx.doi.org/10.1021/cb300323q
- <sup>6</sup>Parida, K., Sahu, N., Mohapatra, P., & Scurrrell, M. (2010). Low temperature CO oxidation over gold supported mesoporous Fe-TiO<sub>2</sub>. *Journal of Molecular Catalysis A: Chemical*, 319(1-2), 92-97. doi:10.1016/j.molcata.2009.12.005
- <sup>7</sup>Zecchina, A., Bordiga, S., Spoto, G., Marchese, L., Petrini, G., Leofanti, G., & Padovan, M. (1992). Silicalite characterization. 1. Structure, adsorptive capacity, and IR spectroscopy of the framework and hydroxyl modes. *The Journal of Physical Chemistry*, 96(12), 4985-4990. doi:10.1021/j100191a047
- <sup>8</sup>Miller, J. E., Gonzales, M. M., Evans, L., Sault, A. G., Zhang, C., Rao, R., . . . King-Smith, D.

(2002). Oxidative dehydrogenation of ethane over iron phosphate catalysts. *Applied Catalysis A: General*, 231, 281-292. Retrieved April 21, 2019.

<sup>9</sup>Dai, H. X., Ng, C. F., & Au, C. T. (2000). Perovskite Type Halo-oxide  $\text{La}_{1-x}\text{Sr}_x\text{FeO}_{3-\delta}\text{X}_\sigma$  (X = F, Cl) Catalysts Selective for the Oxidation of Ethane to Ethene. *Journal of Catalysis*, 189, 52-62. Retrieved April 21, 2019.

Appendix

Appendix A. Lattice Parameter Calculations

	$2\theta$	$\theta$	radians	$\sin\theta$	d	h	k	l	Lattice Parameter	V (nm <sup>3</sup> )	V (Å <sup>3</sup> )
1:50	23.2	11.6	0.202	0.201	0.383	1	5	0	<b>2.012 a</b>	4.306	4305.587
	24	12	0.209	0.208	0.371	5	1	1	<b>1.953 b</b>		
	24.45	12.225	0.213	0.212	0.364	2	5	0	<b>1.096 c</b>		
1:50 Calcined	23.2	11.6	0.202	0.201	0.383	1	5	0	<b>1.934 a</b>	6.339	6339.323
	24.05	12.025	0.210	0.208	0.370	5	1	1	<b>1.956 b</b>		
	24.55	12.275	0.214	0.213	0.363	2	5	0	<b>1.676 c</b>		
1:200	23.2	11.6	0.202	0.201	0.383	1	5	0	<b>2.054 a</b>	3.902	3902.215
	23.95	11.975	0.209	0.207	0.372	5	1	1	<b>1.951 b</b>		
	24.4	12.2	0.213	0.211	0.365	2	5	0	<b>0.973 c</b>		
1:200 Calcined	23.25	11.625	0.203	0.202	0.383	1	5	0	<b>1.970 a</b>	4.977	4977.182
	24.05	12.025	0.210	0.208	0.370	5	1	1	<b>1.950 b</b>		
	24.55	12.275	0.214	0.213	0.363	2	5	0	<b>1.296 c</b>		
1:400	23.2	11.6	0.202	0.201	0.383	1	5	0	<b>2.012 a</b>	4.306	4305.587
	24	12	0.209	0.208	0.371	5	1	1	<b>1.953 b</b>		
	24.45	12.225	0.213	0.212	0.364	2	5	0	<b>1.096 c</b>		
1:400 Calcined	23.2	11.6	0.202	0.201	0.383	1	5	0	<b>1.972 a</b>	5.062	5061.579
	24	12	0.209	0.208	0.371	5	1	1	<b>1.954 b</b>		
	24.5	12.25	0.214	0.212	0.363	2	5	0	<b>1.313 c</b>		

## Appendix B. Conversion Values.

<b>Time (min)</b>	<b>1:50</b>	<b>1:75</b>	<b>1:100</b>	<b>1:200</b>	<b>1:400</b>
5	1.53263	3.299398	4.297425	2.974341	-3.28396
25	4.765076	6.875177	7.879484	6.952776	4.195827
45	4.816462	6.717228	7.800789	6.747492	4.231565
65	5.051688	6.73741	7.71199	6.562368	4.131792
85	5.262594	6.771903	7.764594	6.456788	4.117975
105	5.366639	6.808395	7.762386	6.376507	4.076488
125	5.453447	6.811051	7.752936	6.284291	4.080572

## Appendix C. Selectivity Values.

<b>Time (min)</b>	<b>1:50</b>	<b>1:75</b>	<b>1:100</b>	<b>1:200</b>	<b>1:400</b>
5	60.22596	66.77216	63.14786	66.40833	68.61082
25	73.38317	68.66922	62.71453	68.05833	71.5737
45	74.98344	69.81337	62.97894	68.07647	71.65719
65	78.66251	69.75857	64.15219	68.13369	72.07902
85	79.77743	69.77787	63.7551	67.92738	71.25034
105	80.16038	70.20407	63.76251	67.88907	71.68982
125	81.07308	70.22554	63.97448	67.86612	71.08809

## Appendix D. Rate of Formation Calculations

Average yield of ethylene = (0.0494 mol ethylene)/(mol ethane)

If molecular weight of ethylene is 28.05 g/mol, avg yield = (1.38567 g ethylene)/(mol ethane)

Feed flow = 50 sccm (18% ethane) → 9 sccm ethane

Density of ethane at room temperature and atmospheric pressure = 1.219 kg/m<sup>3</sup>

$$9 \left( \frac{\text{cm}^3}{\text{min}} \right) * 60 \left( \frac{\text{min}}{\text{hr}} \right) * \left( \frac{1}{100} \right)^3 \left( \frac{\text{m}^3}{\text{cm}^3} \right) * 1.219 \left( \frac{\text{kg}}{\text{m}^3} \right) * \left( \frac{1}{30.07} \right) \left( \frac{\text{mol}}{\text{g}} \right) * 1000 \left( \frac{\text{g}}{\text{kg}} \right)$$

$$= 0.0219 \text{ mol ethane/hr}$$

$$\frac{1.38567 \frac{\text{g ethylene}}{\text{mol ethane}} * 0.0219 \frac{\text{mol ethane}}{\text{hr}}}{0.00005 \text{ kg cat}} = 606 \text{ (g ethylene)} * (\text{kg cat})^{-1} * (\text{hr})^{-1}$$